

Research Article

Improvement on Mechanical Properties of Submerged Friction Stir Joining of Dissimilar Tailor Welded Aluminum Blanks

R. Suryanarayanan ¹, V. G. Sridhar,¹ L. Natrayan ², S. Kaliappan ³,
Anjibabu Merneedi ⁴, T. Sathish ², and Alazar Yeshitla ⁵

¹School of Mechanical Engineering, Vellore Institute of Technology, Chennai 600127, Tamil Nadu, India

²Department of Mechanical Engineering, Saveetha School of Engineering, SIMATS, Chennai 602105, Tamil Nadu, India

³Department of Mechanical Engineering, Velammal Institute of Technology, Chennai 601204, Tamil Nadu, India

⁴Department of Mechanical Engineering, Aditya College of Engineering, Surampalem 533437, Andhra Pradesh, India

⁵Department of Biotechnology, College of Biological and Chemical Engineering, Addis Ababa Science and Technology University, Addis Ababa, Ethiopia

Correspondence should be addressed to R. Suryanarayanan; suryan237@gmail.com and Alazar Yeshitla; alazar.yeshi@aastu.edu.et

Received 27 June 2021; Revised 13 July 2021; Accepted 21 July 2021; Published 28 July 2021

Academic Editor: Samson Jerold Samuel Chelladurai

Copyright © 2021 R. Suryanarayanan et al. This is an open access article distributed under the Creative Commons Attribution License, which permits unrestricted use, distribution, and reproduction in any medium, provided the original work is properly cited.

Friction stir welding is a solid-state welding method that produces joints with superior mechanical and metallurgical properties. However, the negative effects of the thermal cycle during welding dent the mechanical performance of the weld joint. Hence, in this research study, the joining of aluminum tailor welded blanks by friction stir welding is carried out in underwater conditions by varying the welding parameters. The tensile tests revealed that the underwater welded samples showed better results when compared to the air welded samples. Maximum tensile strength of 229.83 MPa was obtained at 1000 rpm, 36 mm/min. The improved tensile strength of the underwater welded samples was credited to the suppression of the precipitation of the secondary precipitates due to the cooling action provided by the water. The lowest hardness of 72 HV was obtained at the edge of the stir zone which indicated the weakest region in the weld zone.

1. Introduction

Friction stir welding (FSW), a solid welding technique, is employed to produce weldments with superior joint properties when compared to conventional welding methods. Developed in the year 1991 by The Welding Institute, UK, the FSW process has seen a rapid growth in transportation industry especially in high-speed rails, high-speed ferries, aircrafts, and automobiles [1, 2]. The application of tailor welded blanks in automobiles has enhanced the productivity at reduced costs and has a great potential in marine applications [3]. Aluminum alloys such as Al 5083 and Al 6082, marine grade alloys, are used in ship hull and superstructure and extruded stiffeners [4, 5]. Zadpoor et al. [6] studied the mechanical and microstructural characteristics of the tailor welded blanks. Leitão et al. [7] studied the formability of

friction stir welded similar and dissimilar tailor welded blanks of Al 5182-H111 and 6016-T4. Gungor et al. [4] joined Al 5083 H111 and Al 6082-T6 alloys in similar and dissimilar configurations and studied the tensile and fatigue strength of the welded joints. Dragatogiannis et al. [5] achieved superior properties in Al 5083-Al 6082 joint by FSW by incorporating TiC nanoparticles in the weld zone. Peel et al. [8] observed better mechanical properties by placing Al 5083 on the advancing side as it enhanced sufficient material mixing at the stir zone. Anil et al. [9] obtained superior properties in dissimilar joint configuration when compared to similar joint configuration in FSW of Al 5083 and Al 6082. Svensson et al. [10] joined Al 5083 and Al 6082 by FSW and observed precipitates in the weld zone which was the reason of low microhardness. Donatus et al. [11] studied the material flow in dissimilar FSW of Al 5083-

O and Al 6082-T6 and concluded that tool shoulder and pin played a vital role in material transportation and microstructural evolution. Liu et al. [12] observed increased tensile strength in underwater FSW of Al 2219 samples when compared with that of air welded samples.

Yogeshwaran et al. found that welding speed played a significant role in determining the failure zone of the weld joint as the increase in welding speed resulted in narrowing of the softening region [13]. Rui et al. [14] studied the influence of water temperature on mechanical properties of submerged friction stir welded Al 7050 alloys. Mofid et al. [15] observed that rapid cooling action provided by the submerged medium (liquid nitrogen and water) dented the growth of intermetallic compound formation in submerged friction stir welding of Al and Mg alloys. Kokila et al. [16] also observed similar phenomena in underwater FSW of Al and Mg alloys. Rathinasuriyan and Senthilkumar [17] studied the effects of water head on mechanical properties of the underwater FSW of Al 6061 and optimized it along with other process parameters by response surface methodology. Sabari et al. [18] studied the effects of pin profile on mechanical and microstructural properties in submerged friction stir welding of Al 2519-T87 alloy. Rouzbehani et al. [19] observed that water cooling reduced the width of the HAZ layer in the weld zone in submerged friction stir welding of Al 7075 alloys. Wahid et al. [20] concluded that low peak temperatures obtained in submerged friction stir welding due to water cooling resulted in denting of grain growth and dissolution of precipitates that enhanced the strength of the weld joint. Since most of the literatures have reported the joining of Al 5083 and Al 6082 in air conditions, the underwater welding of these two alloys have not been reported in any of the literatures available; hence, an attempt is done to study the tensile properties and microhardness of the underwater friction stir welded samples.

2. Materials and Methods

Aluminum alloys Al 5083 and Al 6082 were cut to required size of $150 \times 80 \times 6$ mm and $150 \times 80 \times 5$ mm using power axe-saw machine and cleaned with acetone to remove dust and oil. The chemical composition and mechanical properties of the alloys are given in Tables 1 and 2, respectively.

The FSW machine, R. V. Machine Tools, 11 kW was employed to join Al 5083 and Al 6082 which were placed on the advancing side (AS) and retreating side (RS), respectively, Figure 1.

A square pin (Figure 2) of H-13 tool steel with tool dimensions of 25 mm shoulder diameter and pin length of 4.7 mm is used to join the blanks based on the results obtained from previous research studies. The square pin tool was selected for the joining the dissimilar Al alloy, as this tool induces sufficient plasticization of the Al alloys due to the increased probe area and also due to the pulsating action of the tool [21].

Six samples were welded under water condition at 29°C and 25 mm water head. The FSW process parameters and the test results are given in Table 3. The weldments were cut to the dimensions of 100×25 mm tensile test specimen

TABLE 1: Chemical composition of aluminum alloys.

Element	Al 5083	Cu	Fe	Mg	Mn	Si	Cr	Al
Wt%		0.1	0.4	4.2	0.4	0.25	0.2	Balance
Element	Al 6082	Si	Fe	Cu	Mn	Cr	Zn	Al
Wt%		0.7	0.4	0.1	0.6	0.2	0.18	Balance

according to ASTM E8M-02 standard and tested at cross-head speed of 1 mm. The hardness test was conducted using ASTM E-92 standard at loading conditions of 200 g for 15 s.

3. Results and Discussion

The mechanical properties of underwater welded samples at different tool rotational speeds are compared. The underwater welded samples possessed high strength than the air welded samples. The samples welded at a constant weld speed of 24 mm/min were observed with tunnel defects. The tunnel defects are formed due to insufficient plasticization and poor material mixing by the tool profile at the specific welding speed [22]. However, the samples welded underwater at 36 mm/min showed better mechanical properties, as shown in Figure 3. The rapid cooling action provided by water resulted in denting the grain growth and formation of fine grains that might have enhanced the mechanical strength. Moreover, the welding temperature during the underwater FSW would have been $<250^\circ\text{C}$, which dented the coarsening of the strengthening precipitate Mg_2Si to enhance the weld strengths of underwater welded samples compared to the air welded samples [23, 24]. The tensile test samples of failed at the weld zone indicating the nugget zone is not in contact with the submerged medium during FSW which resulted in formation of a weaker zone at the nugget region [12]. The tensile strength of the underwater tensile welded samples tends to decrease with increase in tool rotational speed that increases the temperature at the weld zone which resulted in grain growth in the weld zone; hence, the drop in tensile strength is observed [25, 26].

According to Zadapoor et al. [6] the tensile strength of the tailor welded blank is impacted by the change in the stress concentration factor at the nugget zone, which depends on the thickness of the alloy. Since the blanks of two different thicknesses are being welded, the thickness at the weld zone (nugget) is slightly higher than the thickness of Al 6082; therefore, gradual change in thickness of the nugget zone may improve the mechanical properties of the welded sample. Moreover, the joints during tensile testing show heterogeneous plasticization due to their differences in thicknesses. The plastic deformation in the tailor welded samples during the monotonic loading during the tensile test is determined by the following equation.

$$\frac{YS}{UTS} = \frac{T1}{T2} \quad (1)$$

where T1 and T2 are the thickness of the blanks, mm.

According to this criterion, when the ratio of yield strength to ultimate tensile strength is lesser than the ratio of thicknesses, the plastic deformation is said to be concentrated in both the alloys, whereas when the ratio of strengths

TABLE 2: Mechanical properties of aluminum alloys.

Density (kg/cm ³)	Yield strength (MPa)	Ultimate tensile strength (MPa)	Elongation (%)	Alloy
2.66	288	341	23	Al 5083
2.70	143	295	11	Al 6082



FIGURE 1: Submerged FSW set-up.

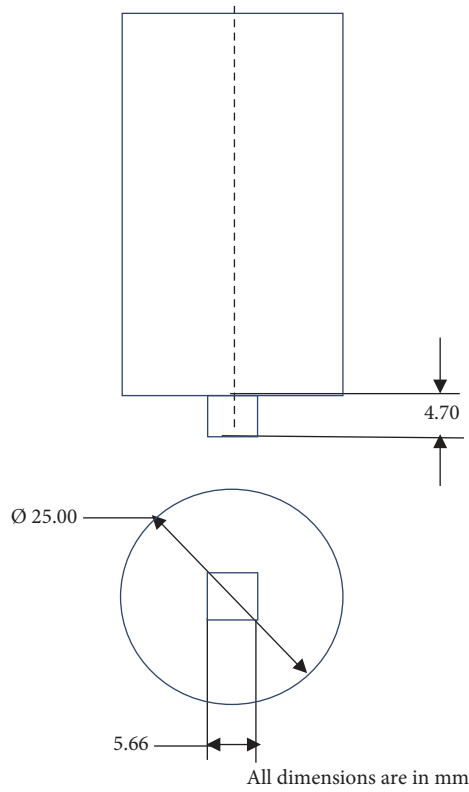


FIGURE 2: Square probe FSW tool.

TABLE 3: Welding parameters for air and underwater FSW with results.

Sample no.	Rotational speed (rpm)	Welding speed, mm (s)	Air welded, yield strength (MPa)	Air welded, ultimate tensile strength (MPa)	Underwater welded, yield strength (MPa)	Underwater welded, ultimate tensile strength (MPa)
1	1000	24	78.99	87	129.68	140.68
2	1200	24	82.25	114.7	134.19	138.28
3	1400	24	87.99	91.82	136.47	148.78
4	1000	36	120	122.18	159.28	229.89
5	1200	36	128	138.78	177.715	182.44
6	1400	36	150.64	154.13	165.626	208.48

is greater than the thickness ratio, then the thinner alloy Al 6082 is plastically deformed. The samples 4 and 5 welded at 36 mm/min agree with the first condition as given in Table 4.

3.1. *Microhardness and Microstructure analysis.* Figure 4 shows the microhardness results; the study was carried out for the sample 4 by application of 200 g load for 15 s. The

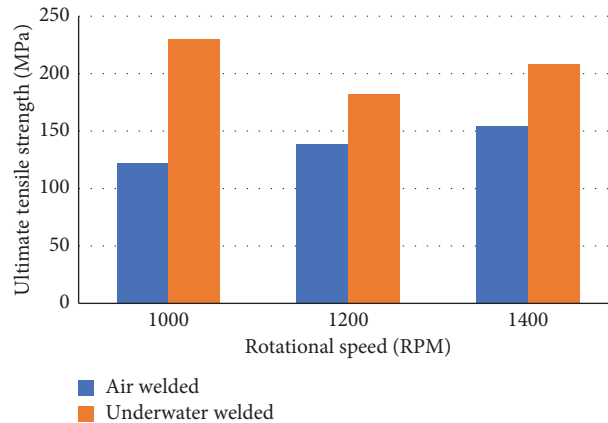


FIGURE 3: Comparison of tensile strength for air welded and underwater welded FSW samples at 36 mm/min.

TABLE 4: Limiting stress ratio criterion.

Sample no.	YS (MPa)	UTS (MPa)	YS/UTS	T ₁ /T ₂
4	159.28	229.89	0.69	0.83
5	165.62	208.48	0.79	0.83
6	177.71	182.44	0.97	0.83

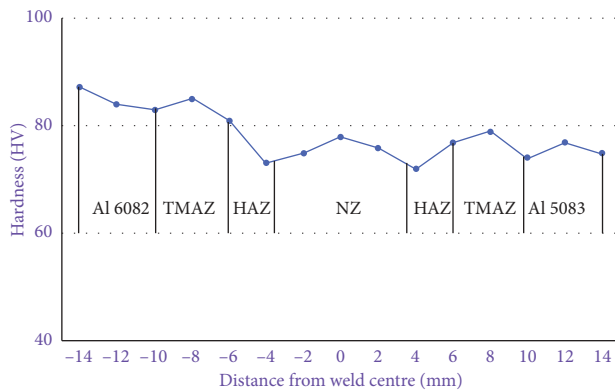


FIGURE 4: Microhardness survey for sample 4, underwater welded specimen joined at 1000 rpm, 36 mm/min.

lowest hardness of 72 HV was observed at the edge of the stir zone (SZ) which indicated the region of failure at the weld zone. The hardness increased at SZ and TMAZ to show that these regions have been strengthened by the water cooling effect.

The microstructure analysis was performed by polishing the sample with different grades of emery sheets and velvet cloth polishing with diamond solution, followed by etching the sample with Keller's reagent. The macrostructure (Figure 5) revealed the mixed flow between the two alloys at the stir zone. The mixed flow indicated that Al 5083 and Al 6082 were able to undergo severe plastic deformation induced by the square tool; however, the complete mixing of the alloys was not achieved [21].

The optical microstructure (Figure 6) revealed the formation of the kissing bond or oxide line with severe plastic deformation (OJLwSPD), which was caused due to the breakdown of the surface oxides. The formation of such a

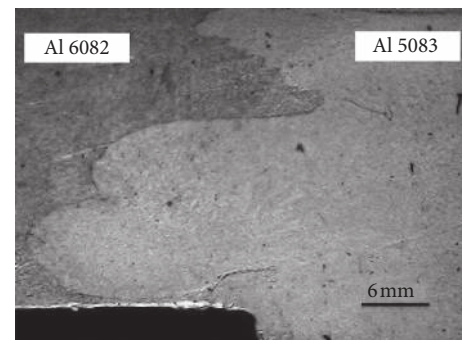


FIGURE 5: Macrostructure of sample 4, underwater welded specimen joined at 1000 rpm, 36 mm/min.

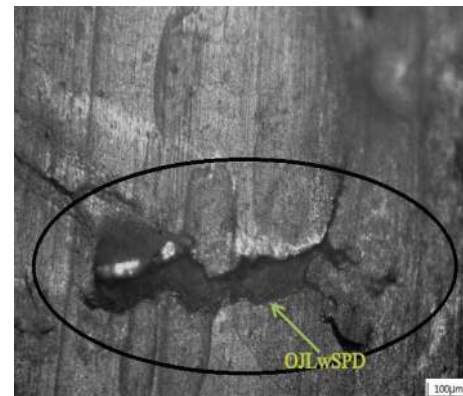


FIGURE 6: Microstructure of sample 4, underwater welded specimen joined at 1000 rpm, 36 mm/min.

defect was due to the insufficient plasticization due to poor stirring of Al 5083 and Al 6082 in underwater conditions.

4. Conclusions

The underwater welded samples perform better mechanically when compared to air welded samples. Maximum tensile strength of 229.83 MPa was obtained at 1000 rpm, 36 mm/min. The rapid cooling action provided by the water resulted in enhancement of the mechanical strength when

compared to air welded samples. The tensile strength of the weld joint decreased with the increase in tool rotational speed that increased the heat input during the welding process that resulted in grain growth at the stir zone. All the six joints welded underwater failed at the weld zone. The lowest hardness of 72 HV obtained for water welded samples was observed at the stir zone indicating the failure zone of tensile-tested joint.

Data Availability

The data used to support the findings of this study are included within the article and are available from the corresponding author upon request.

Disclosure

It was performed as a part of the Employment of College of Biological and Chemical Engineering, Addis Ababa Science and Technology University, Ethiopia.

Conflicts of Interest

The authors declare that there are no conflicts of interest.

Acknowledgments

The authors thank to Vellore Institute of Technology, Chennai, and Saveetha School of Engineering, SIMATS, Chennai, for providing characterization supports to complete this research work.

References

- [1] R. Nandan, T. Debroy, and H. Bhadeshia, "Recent advances in friction-stir welding - process, weldment structure and properties," *Progress in Materials Science*, vol. 53, no. 6, pp. 980–1023, 2008.
- [2] V. Paranthaman, K. S. Sundaram, and L. Natrayan, "Effect of silica content on mechanical and microstructure behaviour of resistance spot welded advanced automotive trip steels," *Silicon*, pp. 1–10, 2021.
- [3] E. E. Feistauer, L. A. Bergmann, L. S. Barreto, and J. F. Dos Santos, "Mechanical behaviour of dissimilar friction stir welded tailor welded blanks in Al-Mg alloys for Marine applications," *Materials & Design*, vol. 59, pp. 323–332, 2014.
- [4] B. Gungor, E. Kaluc, E. Taban, and A. Sik, "Mechanical, fatigue and microstructural properties of friction stir welded 5083-H111 and 6082-T651 aluminium alloys," *Materials and Design*, vol. 56, pp. 84–90, 2014.
- [5] D. A. Dragatogiannis, E. P. Koumoulos, I. A. Kartsonakis, D. I. Pantelis, P. N. Karakizis, and C. A. Charitidis, "Dissimilar friction stir welding between 5083 and 6082 Al alloys reinforced with TiC nanoparticles," *Materials and Manufacturing Processes*, vol. 31, no. 16, pp. 2101–2114, 2016.
- [6] A. A. Zadpoor, J. Sinke, R. Benedictus et al., "Mechanical properties and microstructure of friction stir welded tailor-made blanks," *Materials Science and Engineering: A*, vol. 494, no. 1-2, pp. 281–290, 2008.
- [7] C. Leitao, R. M. Leal, D. M. Rodrigues, A. Loureiro, and P. Vilaça, "Mechanical behaviour of similar and dissimilar AA5182-H111 and AA6016-T4 thin friction stir welds," *Materials & Design*, vol. 30, no. 1, pp. 101–108, 2009.
- [8] M. J. Peel, A. Steuwer, P. J. Withers, T. Dickerson, Q. Shi, and H. Shercliff, "Dissimilar friction stir welds in AA5083-AA6082. Part I: process parameter effects on thermal history and weld properties," *Metallurgical and Materials Transactions A*, vol. 37, no. 7, pp. 2183–2193, 2006.
- [9] K. K. S. Anil, S. M. Murigendrappa, and H. Kumar, "A bottom-up optimization approach for friction stir welding parameters of dissimilar AA2024-T351 and AA7075-T651 alloys," *Journal of Materials Engineering and Performance*, vol. 26, no. 7, pp. 3347–3367, 2017.
- [10] L. E. Svensson, L. Karlsson, H. Larsson, B. Karlsson, M. Fazzini, and J. Karlsson, "Microstructure and mechanical properties of friction stir welded aluminium alloys with special reference to AA 5083 and AA 6082," *Science and Technology of Welding and Joining*, vol. 5, no. 5, pp. 285–296, 2000.
- [11] U. Donatus, G. E. Thompson, X. Zhou, J. Wang, and K. Beamish, "Flow patterns in friction stir welds of AA5083 and AA6082 alloys," *Materials & Design*, vol. 83, pp. 203–213, 2015.
- [12] H. J. Liu, H. J. Zhang, Y. X. Huang, and L. Yu, "Mechanical properties of underwater friction stir welded 2219 aluminum alloy," *Transactions of Nonferrous Metals Society of China*, vol. 20, no. 8, pp. 1387–1391, 2010.
- [13] S. Yogeshwaran, L. Natrayan, G. Udhayakumar, G. Godwin, and L. Yuvaraj, "Effect of waste tyre particles reinforcement on mechanical properties of jute and abaca fiber- epoxy hybrid composites with pre-treatment," *Materials Today: Proceedings*, vol. 37, no. 2, pp. 1377–1380, 2021.
- [14] D. F. Rui, Q. S. Zeng, C. S. Rui, L. Ying, J. L. Hui, and L. Lei, "Improvement of weld temperature distribution and mechanical properties of 7050 aluminum alloy butt joints by submerged friction stir welding," *Materials & Design*, vol. 32, no. 10, pp. 4825–4831, 2011.
- [15] M. A. Mofid, A. Abdollah-Zadeh, F. M. Ghaini, and C. H. Gür, "Submerged friction-stir welding (SFSW) underwater and under liquid nitrogen: an improved method to join Al alloys to Mg alloys," *Metallurgical and Materials Transactions A*, vol. 43, no. 13, pp. 5106–5114, 2012.
- [16] R. V. Kokila, S. R. Radhamohan, L. Natrayan, D. Usha, and V. R. Niveditha, "Guided container selection for data streaming through neural learning in cloud," *Int. J. Syst. Assur. Eng. Manag.*, pp. 1–7, 2021.
- [17] C. Rathinasuriyan and V. S. Senthil, "Modelling and optimization of submerged friction stir welding parameters for AA6061-T6 alloy using RSM," *Metallic Materials*, vol. 54, no. 04, pp. 297–304, 2016.
- [18] S. S. Sree, S. Malarvizhi, and V. Balasubramanian, "Characteristics of FSW and UWFSW joints of AA2519-T87 aluminium alloy: effect of tool rotation speed," *Journal of Manufacturing Processes*, vol. 22, pp. 278–289, 2016.
- [19] R. Rouzbehani, A. H. Kokabi, H. Sabet, M. Paidar, and O. O. Ojo, "Metallurgical and mechanical properties of underwater friction stir welds of Al7075 aluminum alloy," *Journal of Materials Processing Technology*, vol. 262, pp. 239–256, 2018.
- [20] M. A. Wahid, Z. A. Khan, A. N. Siddiquee, R. Shandley, and N. Sharma, "Analysis of process parameters effects on underwater friction stir welding of aluminum alloy 6082-T6," *Proceedings of the Institution of Mechanical Engineers - Part B: Journal of Engineering Manufacture*, vol. 233, no. 6, pp. 1700–1710, 2019.

- [21] R. Palanivel, M. P. Koshy, N. Murugan, and I. Dinaharan, "Effect of tool rotational speed and pin profile on microstructure and tensile strength of dissimilar friction stir welded AA5083-H111 and AA6351-T6 aluminum alloys," *Materials & Design*, vol. 40, pp. 7–16, 2012.
- [22] S. Yogeshwaran, L. Natrayan, S. Rajaraman, S. Parthasarathi, and S. Nestro, "Experimental investigation on mechanical properties of Epoxy/graphene/fish scale and fermented spinach hybrid bio composite by hand lay-up technique," *Materials Today: Proceedings*, vol. 37, no. 2, pp. 1578–1583, 2021.
- [23] V. Paranthaman, K. S. Sundaram, and L. Natrayan, "Influence of SiC particles on mechanical and microstructural properties of modified interlock friction stir weld lap joint for automotive grade aluminium alloy," *Silicon*, pp. 1–11, 2021.
- [24] R. Suryanarayanan and V. G. Sridhar, "Effect of process parameters in pinless friction stir spot welding of Al 5754-Al 6061 alloys," *Metallography, Microstructure, and Analysis*, vol. 9, pp. 1–12, 2020.
- [25] L. Karthikeyan, V. S. Senthilkumar, and K. A. Padmanabhan, "On the role of process variables in the friction stir processing of cast aluminum A319 alloy," *Materials & Design*, vol. 31, no. 2, pp. 761–771, 2010.
- [26] R. Suryanarayanan and V. Sridhar, "Process parameter optimisation in pinless friction stir spot welding of dissimilar aluminium alloys using Multi-start algorithm," *Proceedings of the Institution of Mechanical Engineers - Part C: Journal of Mechanical Engineering Science*, vol. 234, no. 20, pp. 4101–4115, 2020.